Multifunctional electroelastomer roll actuators and their application for biomimetic walking robots

Qibing Pei, Marcus Rosenthal, Ron Pelrine, Scott Stanford, Roy Kornbluh
SRI International, 333 Ravenswood Avenue, Menlo Park, California

ABSTRACT

Dielectric elastomer artificial muscles (electroelastomers) have been shown to exhibit excellent performance in a variety of actuator configurations. By rolling highly prestrained electroelastomer films onto a central compression spring, we have demonstrated multifunctional electroelastomer rolls (MERs) that combine load bearing, actuation, and sensing functions. The rolls are compact, have a potentially high electroelastomer-to-structure weight ratio, and can be configured to actuate in several ways including axial extension and bending, and as multiple degree-of-freedom (DOF) actuators that combine both extension and bending. 1-DOF, 2-DOF, and 3-DOF MERs have all been demonstrated through suitable electrode patterning on a single monolithic substrate. The bending MER actuators can act as leg and knee joints to produce biomimetic walking that is adaptable to many environments. Results of animation and the fabrications of a robot model of a synthetic bug or animal based on the MERs are presented. A new concept for an antagonist actuator for more precise control is introduced.

Keywords: Electroelastomer; multifunctional roll actuator; spring roll; multiple degree-of-freedom actuation; strain sensor; biomimetic walking robot; antagonist actuator

1. INTRODUCTION

New high-performance actuator materials capable of converting electrical energy to mechanical energy or vice versa are needed for a wide range of demanding applications such as mini- and microrobots, biomorphic robots, prosthetic devices, high-performance lightweight motors, pumps, valves, and small-size generators. Diverse candidate materials are under investigation. Most of these materials excel in some measures of performance (such as energy density or strain) but are unsatisfactory in others (such as efficiency and speed of response). For example, single-crystal piezoelectric PZN-PT is perhaps the best-performing inorganic actuator material. It has high actuation pressure (131 MPa), high coupling efficiency, and fast response.[1] However, its maximum strain (1.7%), brittleness, and specific energy density (0.13 J/g) are unattractive for applications where large displacement motion is essential. Electroactive polymers are more attractive in this regard.[2] Conducting polymers such as polypyrrole and polyaniline have high actuation pressure and energy density, but their response speed and coupling efficiency are rather low.[3] Poly(vinylidene fluoride-trifluoroethylene) copolymer is an important actuator polymer.[4] It exhibits reasonably high strain (4%) and elastic energy density (0.3 J/g), though the strain is still not high enough for certain applications where high stroke is essential.

At SRI, we have focused on electroelastomers (electroactive elastomers) with ultrahigh electromechanical strain. Specifically, acrylic copolymer elastomers not only achieve the high and reversible electromechanical strain of 100–380% in area that is possible only with elastomers[5] but also have extraordinarily high specific elastic energy density (3.4 J/g), stress (up to 8 MPa), and electromechanical coupling efficiency (60–90%). This remarkable performance is obtained when the elastomer films are prestrained as much as 25-fold in area. Previously, sturdy and bulky frames were needed to apply this prestrain to the thin polymer films. The frames occupied significantly more space and weighed much more than the polymer films themselves.[6] To address these problems, we have investigated and demonstrated multifunctional electroelastomer rolls (MERs), also called spring rolls, shown in Figure 1.[7] The MERs are multifunctional and reproduce such important functions of natural muscles as motors, sensors, brakes, and springs.[8] They represent an important step in the development of synthetic muscles.

Report Documentation Page

Form Approved
OMB No. 0704-0188

1. REPORT DATE	2. REPORT TYPE	3. DATES COVERED
2003	**N/A**	**-**

4. TITLE AND SUBTITLE	5a. CONTRACT NUMBER
Multifunctional electroelastomer roll actuators and their application for biomimetic walking robots	5b. GRANT NUMBER
	5c. PROGRAM ELEMENT NUMBER
6. AUTHOR(S)	5d. PROJECT NUMBER
	5e. TASK NUMBER
	5f. WORK UNIT NUMBER
7. PERFORMING ORGANIZATION NAME(S) AND ADDRESS(ES) **SRI International, 333 Ravenswood Avenue, Menlo Park, California**	8. PERFORMING ORGANIZATION REPORT NUMBER
9. SPONSORING/MONITORING AGENCY NAME(S) AND ADDRESS(ES)	10. SPONSOR/MONITOR'S ACRONYM(S)
	11. SPONSOR/MONITOR'S REPORT NUMBER(S)

12. DISTRIBUTION/AVAILABILITY STATEMENT
Approved for public release, distribution unlimited

13. SUPPLEMENTARY NOTES
The original document contains color images.

14. ABSTRACT

15. SUBJECT TERMS

16. SECURITY CLASSIFICATION OF:			17. LIMITATION OF ABSTRACT	18. NUMBER OF PAGES	19a. NAME OF RESPONSIBLE PERSON
a. REPORT	b. ABSTRACT	c. THIS PAGE			
unclassified	**unclassified**	**unclassified**	**UU**	**10**	

Standard Form 298 (Rev. 8-98)
Prescribed by ANSI Std Z39-18

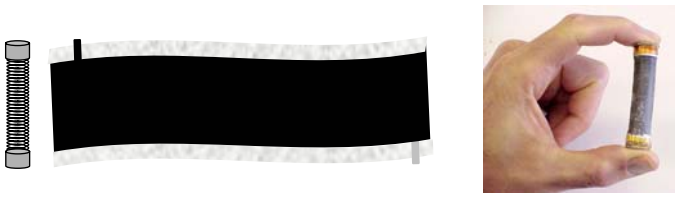

Figure 1: 1-DOF MER. Left: Schematic drawing of fabrication process. Two prestrained films are rolled around a compressed central spring. The black area is the electroded area (on both sides of the film). Right: A spring roll with axial extension strain.

Previously, 3-DOF MERs were demonstrated, with limited performance. In this paper we report our recent progress on 2- and 3-DOF MERs, and the demonstration of a legged robot model using a 2-DOF MER as each of the robot's six legs. Finally, we propose a new concept for an antagonist actuator that will enable more precise control of movement.

2. 2-DOF SPRING ROLL ACTUATORS

Actuator Fabrication: The fabrication of 2-DOF MERs was similar to that of 1-DOF MERs, except that the electrodes were patterned. Two acrylic films were prestrained, coated with compliant carbon-based electrodes that were patterned as shown in Figure 2, laminated together, and rolled around a compression spring. Figure 2 illustrates the fabrication process. When the roll was free standing, the compressed spring held the acrylic films in high circumferential and axial prestrain. About 10–40 layers were stacked in the roll. The electrodes on each layer span < 180° around the circumference. The electrodes on each side of the roll align radially across the layers and are electrically connected. Figure 2 also shows a fabricated 2-DOF roll.

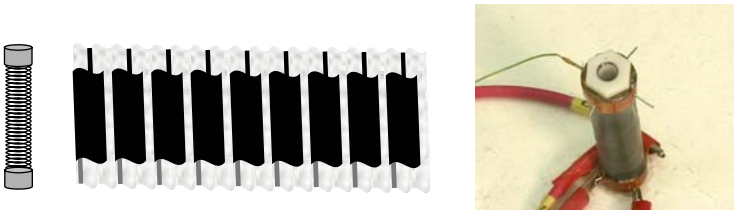

Figure 2: Two-DOF MER. Left: Schematic drawing of fabrication process. Two prestrained films are rolled around a compressed central spring. The electroded areas are prepatterned such that in the spring roll they align radially on the two opposite sides of the roll. Right: Two-DOF spring roll with four sides individually actuated for bending and axial extension.

Bending, Stroke, and Force: The 2-DOF MER shown in Figure 2 is 9 cm in total length and 2.3 cm in diameter, and weighs 29 g. In order to rate the performance of the MERs, we measured their bending angle, lateral displacement, and lateral force. The maximum achieved bending angle between the two ends of the roll was 60° when only one side of the roll was actuated at 5.9 kV. The lateral displacement (movement of one end of the roll with respect to the roll's central axis when unactivated) was 3.3 cm at 5.5 kV. A chart showing the bending angle and lateral displacement vs. voltage is shown in Figure 3. The lateral force was measured by fixing one end of the bending roll, while the other end of the roll was laterally attached to a force gauge. The reading was taken when one side was actuated. The maximum lateral force measured was 1.68 N at 7.7 kV. At 6 kV, when the MER could be repeatedly operated without failure, the lateral force was 1.15 N. When both sides of the roll were actuated, the roll behaved like a 1-DOF spring roll, with longitudinal stroke and force slightly less than those of a 1-DOF roll, due to the inactive areas between the opposite electrodes.

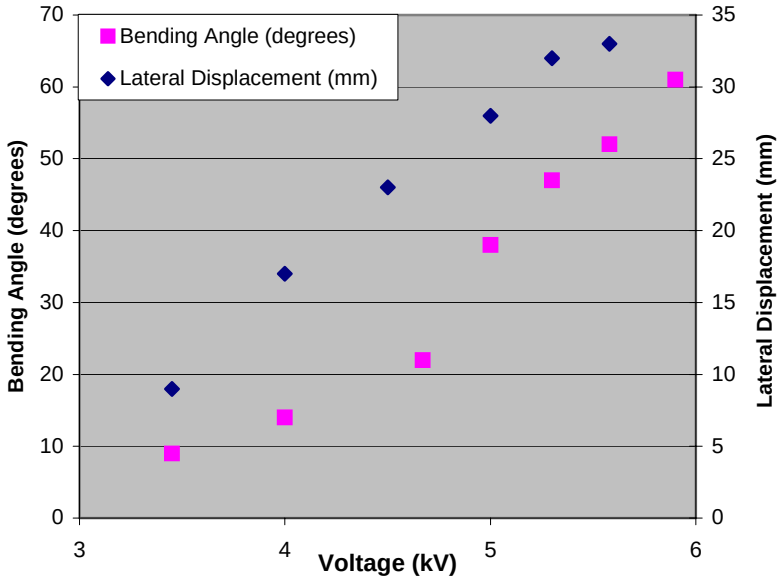

Figure 3: Bending Angle and Lateral Displacement of a 2-DOF MER.

3. TWO-DOF SPRING ROLL FOR POSITION SENSING

The deformation of a 2-DOF MER is a combination of axial extension and bending. Candidate parameters to sense the mechanical deformation of electroelastomers include the capacitance of the electroelastomers, the resistance of the compliant electrodes, and the resistance of the electroelastomers. We did an analysis to correlate the deformation with the capacitance of the electrodes. To obtain the relationship between the measured capacitance and the axial extension and bending, a schematic drawing (Figure 4 [left]) shows the structure of a bending roll. Several assumptions are made:

1. The curvature of the bent roll is constant.
2. The cross-sections of the rolls, including the end surfaces, are circular and perpendicular to the axis of the roll. The diameter of the roll, *d*, is constant.
4. The arc defined by h_θ (the arc length of the roll at an angle θ relative to the diameter and perpendicular to the roll radius *R* has the same angle ϕ as the arc defined by *h* (the arc length of the center of the roll). That is, we are approximating $\phi_h = \phi_{h\theta}$.
5. Between points a and b, θ defines the section of the roll that is active (coated with an electrode that has a voltage potential across it).

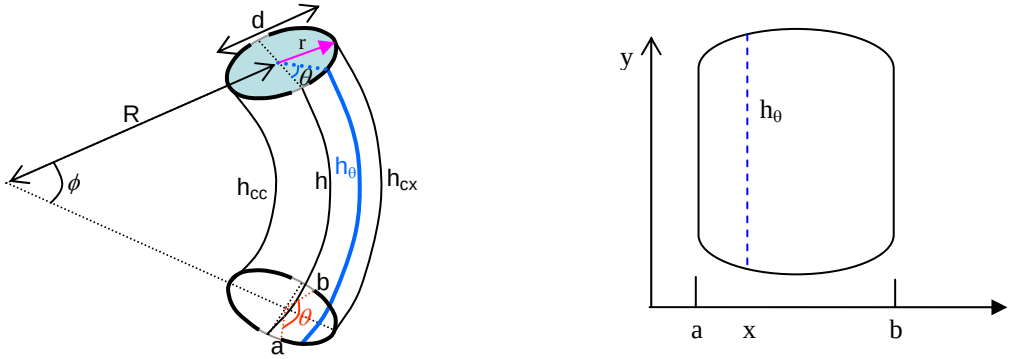

Figure 4: Structure of a bending 2-DOF spring roll. (Left) Schematic drawing of a bending 2-DOF MER. (Right) A roll is unfolded to facilitate the integration of the surface area.

The roll length at the central point is

$$h = R \cdot \phi \tag{1}$$

$$h_\theta = (R + r \cdot \sin\theta) \cdot \phi \tag{2}$$

The outmost and longest length of the roll is at the crest of the convex ($\theta = \pi/2$) and equals

$$h_{cv} = (R + r) \cdot \phi \tag{3}$$

The innermost and shortest length of the roll is at $\theta = 3\pi/2$, the trough of the concave, and equals

$$h_{cc} = (R - r) \cdot \phi \tag{4}$$

To derive the active area of the bent roll, the bent cylinder is unfolded to a plane as shown in Figure 4 (Right). The active area

$$\begin{aligned} A &= \int_a^b h_\theta \bullet dx \\ &= \int_a^b (R + r \bullet \sin\theta) \bullet \phi \bullet dx \end{aligned} \tag{5}$$

For the convex active area, since

$$a = \frac{1}{2}(\pi - \theta t) \bullet r \tag{6}$$

$$b = \frac{1}{2}(\pi + \theta t) \bullet r \tag{7}$$

$$\begin{aligned} A_{cx} &= \int_{(\pi-\theta t)/2}^{(\pi+\theta t)/2} (R + r \bullet \sin\theta) \bullet \phi \bullet r \bullet d\theta \\ &= R \bullet \phi \bullet r \bullet \theta t + 2 \bullet r^2 \bullet \phi \bullet \cos\left(\frac{\pi - \theta t}{2}\right) \end{aligned} \tag{8}$$

Similarly, the concave active area is

$$\begin{aligned} A_{cc} &= \int_{(3\pi-\theta t)/2}^{(3\pi+\theta t)/2} (R + r \bullet \sin\theta) \bullet \phi \bullet r \bullet d\theta \\ &= R \bullet \phi \bullet r \bullet \theta t - 2 \bullet r^2 \bullet \phi \bullet \cos\left(\frac{\pi - \theta t}{2}\right) \end{aligned} \tag{9}$$

The thickness of the acrylic film

$$T = \frac{V}{A_{total}} = \frac{V}{2\pi \bullet r \bullet h} \tag{10}$$

wherein V is the volume of acrylic film and is assumed constant during actuation. When the roll is at rest, the original thickness of the acrylic film is

$$T_o = \frac{V}{A_o} = \frac{V}{2\pi \bullet r \bullet h_o} \tag{11}$$

In this equation h_o is the original length of the roll at rest.

Therefore the thickness of acrylic film during actuation is

$$T = \frac{h_o}{h} \bullet T_o \tag{12}$$

Assuming that the roll has *n* active layers stacked together, the total capacitance of the convex active layers is

$$\begin{aligned} C_{cx} &= n \bullet \varepsilon_o \bullet \varepsilon \bullet \frac{A_{cx}}{T} \\ &= n \bullet \varepsilon_o \bullet \varepsilon \bullet \frac{R \bullet \phi \bullet r \bullet \theta t + 2 \bullet r^2 \bullet \phi \bullet \cos(\frac{\pi - \theta t}{2})}{T_o \bullet {}^{h_o}\!/_{h}} \end{aligned} \tag{13}$$

The total capacitance of the concave active layers is

$$\begin{aligned} C_{cc} &= n \bullet \varepsilon_o \bullet \varepsilon \bullet \frac{A_{cc}}{T} \\ &= n \bullet \varepsilon_o \bullet \varepsilon \bullet \frac{R \bullet \phi \bullet r \bullet \theta t - 2 \bullet r^2 \bullet \phi \bullet \cos(\frac{\pi - \theta t}{2})}{T_o \bullet {}^{h_o}\!/_{h}} \end{aligned} \tag{14}$$

The sum of the capacitances is

$$C_{cx} + C_{cc} = 2n \bullet \varepsilon_o \bullet \varepsilon \bullet \frac{R \bullet \phi \bullet r \bullet \theta t}{T_o \bullet {}^{h_o}\!/_{h}} = \frac{h^2}{{h_o}^2} \bullet [C_{cx} + C_{cc}]_o \tag{15}$$

wherein $[C_{cx} + C_{cc}]_o$ is the total capacitance of the roll at rest (zero strain and bending).

The difference of the capacitance of the outer and inner layers is

$$\begin{aligned} C_{cx} - C_{cc} &= 4n \bullet \varepsilon_o \bullet \varepsilon \bullet \frac{\phi \bullet r^2 \bullet \cos(\frac{\pi - \theta t}{2})}{T_o \bullet {}^{h_o}\!/_{h}} \\ &= \frac{2\phi \bullet r \bullet h \bullet \cos(\frac{\pi - \theta t}{2})}{{h_o}^2 \bullet \theta t} \bullet [C_{cx} + C_{cc}]_o \end{aligned} \tag{16}$$

To use the roll as a sensor, one needs to measure the capacitance of the two bending sides, C_{cx} and C_{cc}. From the measured value, the position of the roll can be determined through the axial length and bending angle.

The axial length of the roll is

$$h = h_o \sqrt{\frac{[C_{cx} + C_{cc}]}{[C_{cx} + C_{cc}]_o}} \tag{17}$$

The bending angle is

$$\phi = \frac{h_o \bullet \theta t}{2r \bullet \cos(\frac{\pi - \theta t}{2})} \bullet \frac{[C_{cx} - C_{cc}]}{\sqrt{[C_{cx} + C_{cc}] \bullet [C_{cx} + C_{cc}]_o}} \tag{18}$$

We are currently verifying the validity of Equations 17 and 18. Preliminary measurements of 2-DOF MER rolls showed that the capacitance of the nonactivated roll is 3.51 nF on each side. Figure 5 shows the capacitance of the electrode on the outside versus the end deflection of the roll. The abnormity at 0 deflection is due to measurement accuracy. More experimental testing is underway to correlate the roll deflection and capacitance change expressed by the equations.

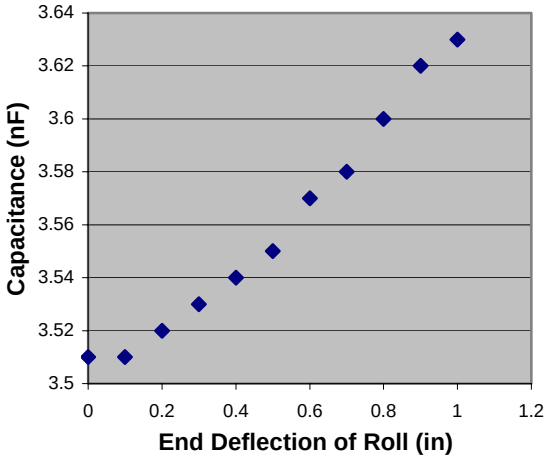

Figure 5: Capacitance (*Ccx*) change of a 2-DOF MER during bending.

4. WALKING ROBOT ENABLED BY 2-DOF SPRING ROLLS

A laboratory robot model was fabricated to demonstrate the unique characteristics of the 2-DOF spring rolls. The robotic system shown in Figure 6, dubbed MERbot, is a simple robot that contains six spring rolls, a hexagonal frame (chassis), and wires. Its dimensions are 18 cm × 18 cm × 10 cm and its weight is 292 g. The power and controls are tethered to the robot. The robot moves with a dual tripod gait, which requires only four input controls: two controls for bending each tripod forward, and two controls for bending each tripod backward.

Figure 6: MERbot, a robot using a 2-DOF spring roll as each of its six legs.

The speed of the MERbot was measured as a function of frequency. The experimental result is shown in Figure 7. The two sets of data at 4.5 kV represent the improvement gained by tuning the robot. In order to tune the robot, we used spacers to raise the legs that were slightly shorter than others to ensure equal weight distribution. The current maximum speed of the MERbot is 13.6 cm/s at 7 Hz with 5.5 kV of driving voltage.

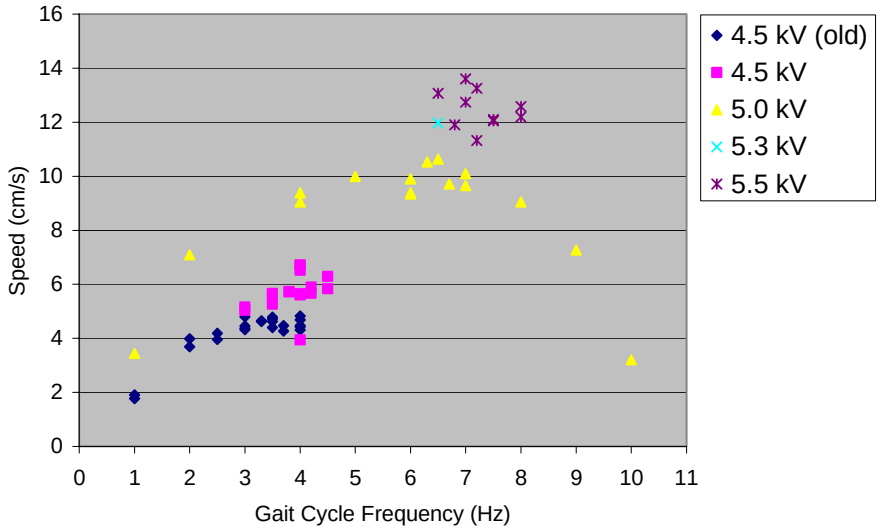

Figure 7: Speed of MERbot at various driving frequencies.

The MERbot was only a proof-of-concept robot and has by no means been optimized. Its performance can be improved in a number of ways. For example, the MERbot was driven at voltages up to 5.5 kV in order to ensure that the MER legs were operated in a safe range (free from breakdown). The typical breakdown voltage of the MERs is 6.5–7.5 kV. So, the stroke of each stride can be doubled, which could increase the robot's speed to about 26 cm/s, assuming that traction causes only minor dragging.

5. 3-DOF SPRING ROLLS

The 3-DOF MERs were fabricated in a similar manner, except that the electrodes were patterned on all four sides of a roll. Each electrode spans 90° of the roll's circumference. Two adjacent electrodes of a 3-DOF spring roll can be actuated together to obtain lateral displacement similar to that of a 2-DOF spring roll. The 3-DOF spring roll is able to bend along 2 axes in addition to longitudinal extension. When two electrodes were actuated, the lateral displacement was 3.5 cm at 5.15 kV. When one electrode of the 3-DOF MER was actuated, the lateral displacement was 2.7 cm at 5.75 kV.

In one test, a spring roll was attached to a joystick to make it easy to bend in any direction. In a separate test the roll was programmed with LabVIEW to actuate the four electrodes in sequences, producing either a circular motion or a figure-eight pattern. In the circular motion, the roll was driven to spin at 240 rpm in a 6 cm diameter circle. In future study, the 3-DOF spring rolls will be integrated into MERbot to enable it to move in any direction without repositioning.

6. ANTAGONIST ACTUATOR CONCEPT

The design of multi-DOF spring rolls may be extended to develop an antagonist actuator. The film is held in preload by means of a lever (spine disc) about a central shaft, as opposed to a central compression spring. The fabrication process is similar to that of the MERs as shown in Figure 8. The principle of preloading is similar to the way a flexor and extensor muscles function as an antagonist pair in biological systems. Figure 10 shows how the tibialis and soleus muscles have opposite effects and function as an antagonist pair. Similarly, in the MER antagonist actuator, the change in muscle length of one side of the roll due to activation is balanced out by the prestrain of the inactive muscle on the other side. This motion will produce a change in the angle of the end segment (joint) as shown in Figure 9.

Figure 8: Assembly of an antagonist actuator.

The left shows the film with patterned electrodes. On the right is the central shaft with spine discs

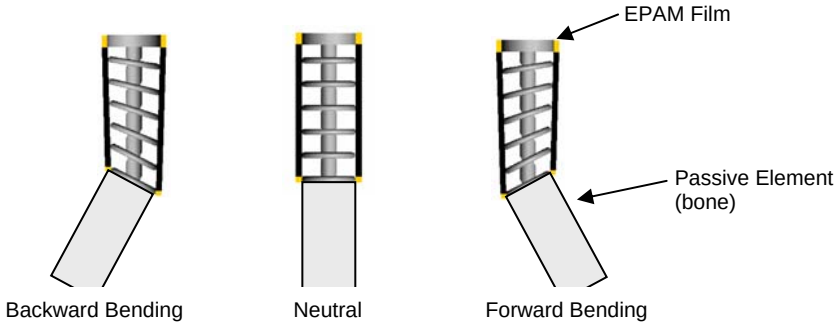

Figure 9: Uniaxis antagonist actuator motion states.

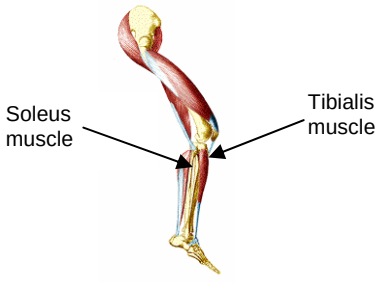

Figure 10: Human leg muscles.

The performance of the uniaxis antagonist actuator is similar to that of the 2-DOF MER spring rolls, but, a hinge joint with a rigid shaft would make more precise control possible. If the strain of the actuated muscle is known, then the angle of the end segment can be determined. A passive element can be attached to the end of the joint actuator for amplified motion. The motion that is produced is similar to that of an arm or leg joint. Since the film is prestrained, the force output by the actuator is proportional to the number of layers of the device. Further designs of the antagonist actuator can enable 3-DOF movement via spine discs that are mounted as ball joints instead of hinge joints.

7. SUMMARY AND REMARKS

Multi-DOF electroelastomer roll actuators (MERs or spring rolls) are easy to fabricate, compact, multifunctional, and mechanically robust. We believe that multi-DOF MERs represent a radically new actuation technology and can enable a number of unique applications in the following areas.

Locomotion: Spring roll legs can be directly attached to a robot chassis, eliminating the need for more complicated "hip" or "knee" joints. Such a robot could walk in any direction equally well. In addition, the serial connection of 2-DOF or 3-DOF spring rolls could result in high-performance serpentine robots. An entire serpentine robot could be made from a monolithic piece of polymer suitably patterned and configured into a high-DOF MER.

Manipulation: Multi-DOF spring rolls simplify manipulation mechanisms, thanks to their fewer joints and less wiring in cramped spaces. The ability to sense strain improves control and hence would enable a robot to pick up and handle delicate objects. A multi-DOF spring roll could be designed to grasp items much as an elephant's trunk does.

Massive parallel systems: Hundreds of spring rolls could be placed in an array for either locomotion (like a starfish) or object manipulation (like an air table).

ACKNOWLEDGEMENTS

Much of this work was sponsored by the Synthetic Multifunctional Materials Program of the Defense Advanced Research Projects Agency (DARPA), under ONR Contract No. N00014-00-C-0497. The authors would like to thank their co-workers, particularly Mr. Neville Bonwit, Mr. Don Czyzyk, Ms. Shari Shepherd, and Dr. Prasanna Mulgoankar, for technical support and valuable discussions.

REFERENCES

1. S. Park and T. Shrout, "Ultrahigh strain and piezoelectric behavior in relaxor-based ferroelectric single crystals," *J. Applied Physics*, **82**, pp. 1804–1811, 1997.

2. R. Baughman, L. Shacklette, R. Elsenbaumer, E. Pichta, and C. Becht, 1990, "Conducting polymer electromechanical actuators," in *Conjugated Polymeric Materials: Opportunities in Electronics, Optoelectronics and Molecular Electronics*, eds. J. L. Bredas and R. R. Chance, Kluwer Academic Publishers, The Netherlands, pp. 559–582, 1990; T. Furukawa and N. Seo, "Electrostriction as the origin of piezoelectricity in ferroelectric polymers," *Jpn. J. Applied Physics*, **29** (4), pp. 675–680, 1990; H. Tobushi, S. Hayashi, and S. Kojima, "Mechanical properties of shape memory polymer of polyurethane series," *JSME International J*., Series I, **35** (3), 1992; R. Pelrine, J. Eckerle, and S. Chiba, "Review of artificial muscle approaches," *Proc. Third Intl. Symposium on Micro Machine and Human Science*, Nagoya, Japan, 1992; M. Zhenyl, J. I. Scheinbeim, J. W. Lee, and B. A. Newman, "High field electrostrictive response of polymers," *J. Polymer Sciences*, Part B—*Polymer Physics*, **32**, pp. 2721–2731, 1994; M. Shahinpoor, "Micro-electro-mechanics of ionic polymer gels as electrically controllable artificial muscles," *J. Intelligent Material Systems and Structures*, **6**, pp. 307–314, 1995.

3. Q. Pei and O. Inganas, " Electrochemical applications of the bending beam method. 1. Mass transport and volume changes in polypyrrole during redox," *J. Physical Chemistry*, **96**, pp. 10507–10514, 1992; Q. Pei, O. Inganas, and I. Lundstrom, "Bending bilayer strips built from polyaniline for artificial electrochemical muscles," *Smart Materials and Structures*, **2**, pp. 1–6, 1993.

4. Q. Zhang, Q. V. Bharti, and X. Zhao, "Giant electrostriction and relaxor ferroelectric behavior in electron-irradiated poly(vinylidene fluoride-trifluorethylene) copolymer," *Science*, **280**, pp. 2101–2104, 1998; Zhang, Q., H. Li, M. Poh, Z.-Y. Cheng, F. Xia, and C. Huang, "An All Organic Composite Actuator Material with a High Dielectric Constant," *Nature*, **419**, 284–287, 2002.

5. R. Pelrine, R. Kornbluh, Q. Pei, and J. Joseph, "High-speed electrically actuated elastomers with over 100% strain," *Science*, **287**, pp. 836–839, 2000.

6. K. Meijer, M. Rosenthal, and R.J. Full, "Electro-active polymers: how muscle-like are they?" *Proc. SPIE*, **4329**, 2001.

7. Q. Pei, S. Stanford, M. Rosenthal, R. Pelrine, R. Kornbluh, K. Meijer, R. Full, "3-D Multifunctional Electroelastomer Actuators and Their Application for Biomimetic Walking Robots," in Smart Structures and Materials 2002: Industrial and Commercial Applications of Smart Structures Technologies, ed. A. McGowan, *Proc. SPIE*, **4698**,

246–253, 2002; Q. Pei, R. Pelrine, S. Stanford, R. Kornbluh, M. Rosenthal, K. Meijer, R. Full, “Multifunctional Electroelastomer Rolls,” *Materials Research Society Symposium Proceedings*, **698**, 165–170, 2002.

8. M. H. Dickinson, C. T. Farley, R. J. Full, M.A.R. Koehl, R. Kram, and S. Lehman, “How animals move: an integrative view,” *Science*, **288**, pp. 100–106, 2000.